# Characterization and quality control of the readout electronics for the readout electronics of the Hodoscope and ICC for the ADAPT experiment

G. DE PALMA(\*) FOR THE APT COLLABORATION

Politecnico di Bari & Dipartimento Interateneo di Fisica "Michelangelo Merlin", INFN Sezione di Bari

Summary. — The "Advanced Particle—astrophysics Telescope" (APT) is a mission concept for a future space-based MeV-TeV observatory, designed to combine a Compton and  $e^+e^-$  pair telescope. To support this mission and check the future capabilities of APT, a small-scale prototype, the "Antartic Demonstrator for APT" (ADAPT), is currently under development and is planned to fly on balloon in Antarctica during the 2026-2027 flight season. Among its subdetectors, ADAPT includes a hodoscope made of four layers of interleaved scintillating fibers coupled to Silicon Photomultipliers (SiPMs), and an Imaging CsI calorimeter, formed by 4 layers of CsI(Na) crystals with crossed WLS fibers readout by SiPMs. A multichannel electronics is essential for these type of detectors: specifically the SMART (SiPM Multichannel ASIC for high Resolution Cherenkov Telescopes) ASIC will be used for the amplification of signals coming from the SiPMs, offering compactness, low cost and a high level of electronic integration.

# 1. - The Advanced Particle Telescope (APT)

The Advanced Particle–astrophysics Telescope (APT) is a planned space-based observatory dedicated to gamma–ray and cosmic–ray (CR) physics. It is designed to operate in orbit around the second Sun–Earth Lagrangian point (L2). Thanks to its multilayer tracker and imaging calorimeter, APT will be capable of detecting gamma rays across a broad energy range, from hundreds of keV up to a few TeV, and will combine a Compton and pair telescope in one single instrument [1]. Characterized by a sensitive area of  $3\,\mathrm{m}\times3\,\mathrm{m}\times2.5\,\mathrm{m}$ , the main features of APT, optimized to achieve the highest possible effective area and field of view (FoV) for observation, are:

• 20 layers of 5 mm thick CsI(Na) scintillating tiles, with a crossed wavelength shifting (WLS) fiber readout;

 $<sup>(\</sup>sp{*})$ mailto:gaia.depalma@ba.infn.itgaia.depalma@ba.infn.it

- 20 XY scintillating optical fiber trackers (SOFT) layers, with 1.5 mm interleaved round scintillating fibers;
- Top-bottom symmetry to double the FoV in the L2 orbit;
- A fiber readout on the side of the detector, with a Silicon Photo-Multipliers (SiPMs)-based analog signal digitization.

# 2. - The Antarctic Demonstrator for APT (ADAPT)

The Antarctic Demonstrator for APT (ADAPT) is a prototype high-altitude balloon mission planned for a long-duration flight on a 60 million cubic foot balloon during the 2026-2027 summer window in Antarctica. ADAPT is a scaled-down version of APT, incorporating only 1% of the total amount of material that will be used for APT: while APT will include 20 Imaging CsI Calorimeter layers, each with an area of  $3~m^2$ , ADAPT features 4 ICC layers, each measuring  $45~\rm cm$  on a side. The mission will serve as a proof-of-concept for prompt Compton event reconstruction and localization and will provide real-time positional alerts for gamma-ray transient such as Gamma-ray Bursts (GRB). The ADAPT detector stackup is illustrated in Fig. 1: it consists of four primary detector layers, each comprising an Imaging CsI Calorimeter (ICC) and a scintillating fiber tracker; specifically, it will include [2]:

- SSDs: Silicon Strip Detectors (SSDs) on top of the structure to identify CRs' charge; these elements will enhance the resolution for charge measurement and provide an higher precision in Compton reconstruction for low-energy events;
- *ICCs*: Imaging CsI Calorimeter modules; 4 layers, each one consisting of  $3\times3$  tiles of  $15~\rm cm \times 15~\rm cm \times 15~\rm mm$  of CsI(Na) crystals, with crossed  $2\times2~\rm mm^2$  WLS fibers and a SiPM readout to measure the position of the interaction; moreover, they will present SiPM-based CsI edge detectors for triggering and charge measurements. One single layer of edge detector can be seen in Fig.2; these elements are a specific feature of ADAPT, and have been added in order to maximize the capture of optical photons that might have escaped the fibers;
- *Hodoscope*: 4 layers of X-Y crossed scintillating fiber tracker modules, with interleaved 1.5 mm scintillating fibers and a SiPM readout;
- Tail Counters: 4 layers of CsI modules equipped with only edge detector readouts for energy measurements.
- Anti-Coincidence Detector (ACD): a segmented anti-coincidence module, specifically developed and designed to discriminate gamma-rays against the charged Cosmic-Ray background. It is composed by 36 upper tiles plus 24 side tiles made of plastic scintillator, the EJ200, arranged in order to envelop the whole ADAPT instrument.

### 3. - Readout electronics for ICC and Hodoscope

The SiPM readout for both the Hodoscope and the ICC will involve a large number of channels; therefore, a multichannel ASIC approach is essential to ensure compact and

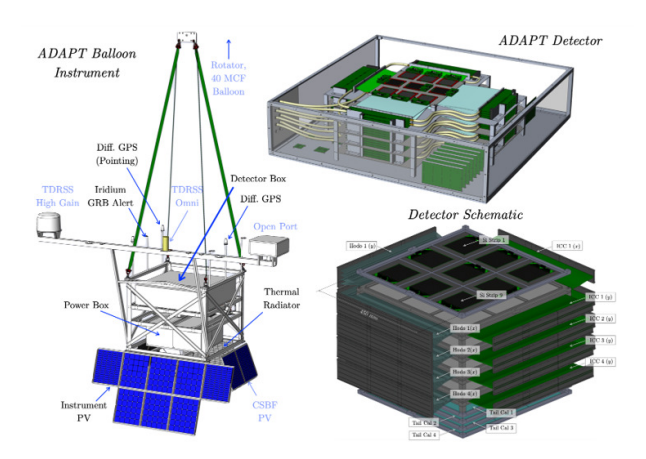


Fig. 1. – ADAPT balloon instrument: on the left, scheme of the whole equipped balloon, on the right a focus on the ADAPT instrument, with a schematic of the stackup on the bottom left part

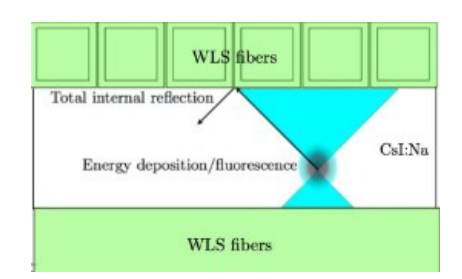


Fig. 2. – Single ICC layer; the totally internally reflected (TIR) optical light propagation and detection are highlighted in blue; moreover, both the edge detector and WLS SiPMs have been included in each layer, the former on the left side and the latter on the right side, both in grey

low-power electronics. Specifically, the readout system will employ Hamamatsu SiPMs coupled to wavelength shifting (WLS) or scintillating fibers, along with multiplexing boards to sum up signals from three SiPMs to reduce the number of readout channels. Moreover, the signal chain will include a pre-amplification stage based on the 16-channel SMART ASIC [3] followed by a waveform digitizer for the SiPM signals acquisition. The main features of the ADAPT readout electronics for these two main instrument can be summarized as it follows:

- Hamamatsu SiPMs coupled to WLS or scintillating fibers;
- Multiplexing boards to sum up 3 SiPMs and reduce the number of readout channels;
- Pre-amplification stage based on the 16-channel SMART ASIC [4];
- Waveform digitizer to readout SiPMs' signals waveforms.
- **3**<sup>1</sup>. The SMART ASIC. The SMART (SiPM Multichannel ASIC for high Resolution Cherenkov Telescopes) ASIC is a 16-channel pre-amplifier, developed in a 35  $\mu$ m Si-Ge

technology by the electronics Computer Aided Design (CAD) service of INFN Bari [3]. It consists of 16 channels, each one featuring a trans-impedance amplifier with two paths: a fast path, specifically designed and optimized for photon counting, and a slow path developed for SiPM mean current measurements. The former is equipped with a signal shaping filter followed by the output buffer, the latter benefits from a low-pass amplifier to measure the mean current of the SiPM with a 20 nA resolution. Finally, the slow path output is sent to an internal Successive-Approximation-Register (SAR) 10-bit analog-to-digital converter (ADC) through an analogue multiplexer.

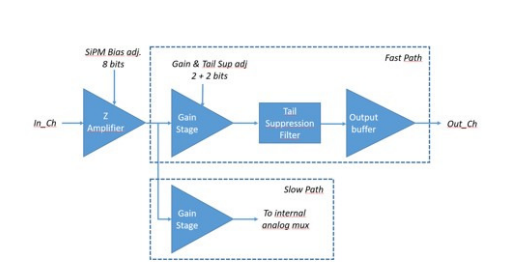




Fig. 3. - Left: internal structure of each SMART channel right: the SMART ASIC

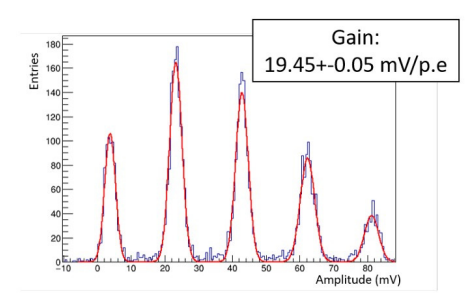
**3**<sup>•</sup>2. *Hodo SMART Board*. – A custom electronics board was designed to serve as preamplification stage for SiPMs on the Hodoscope. These boards host 3 SMART ASICs, for a total of 48 readout channels. A total of 32 boards are necessary to readout the full ADAPT instrument.

The SMART ASIC has customizable parameters that allow adjustment of the preamplifier Gain (R), Bandwidth (C) and Pole ZERO compensation (PZ); moreover, the SiPM bias level can be adjusted for each channel  $(V_{DAC})$ .

In order to validate the performance of the SMART pre-amplification stage, we first conducted a prototyping phase. The tests were performed coupling the SMART inputs to Hamamatsu SiPMs S13360-2050VE  $2\times2$  mm² operated at 57 V and illuminated with a pulsed LED. The output pulses were then acquired through a Lecroy HDO6104B oscilloscope. In Fig.4 we show the amplitude distribution (left) and single photoelectron pulse (p.e.). As a result, the obtained gain was  $19.45\pm0.05mV/p.e.$  with a signal-to-noise ratio (SNR) of about 9. Next, from the single p.e. waveform the Full Width at Half Maximum (FWHM) and the recovery time were extracted by performing a gaussian and then exponential fit. Several SMART configurations were tested.

After this first phase, a total of 40 Hodoscope SMART boards (32+8 spare) were produced and tested. Also in this case, the SMART inputs were coupled to an array of Hamamatsu SiPMs S13360-2050VE  $2\times2$  mm<sup>2</sup> operated at 57 V and illuminated with a pulsed LED. For each channel, the mean waveform was calculated, and then both a Gaussian and exponential fit were performed to obtain the FWHM and recovery time; the results confirmed the expected behavior for all the tested boards. In Fig.5 it is possible to see the distributions of the FWHM and recovery time for each channel at three specific configurations.

**3**<sup>·</sup>3. CsI SMART Board. – The CsI SMART Board was specifically designed to read the signals coming from the ICC SiPMs. These boards host 5 SMART ASICs for a total



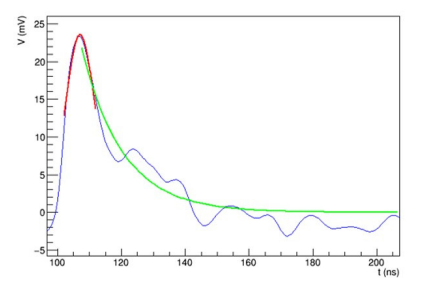
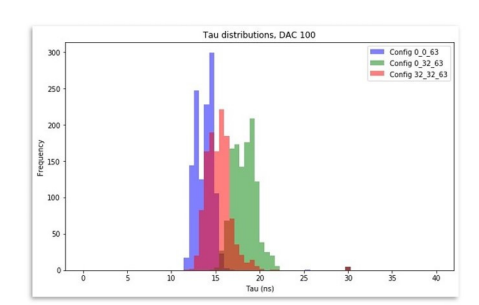


Fig. 4. – Left: amplitude distribution obtained from SMART output signals coupled to a  $2\times2$  mm2 S13360-2050VE Hamamatsu SiPM operated at 57 V. Right: single photoelectron pulse measured in the same conditions



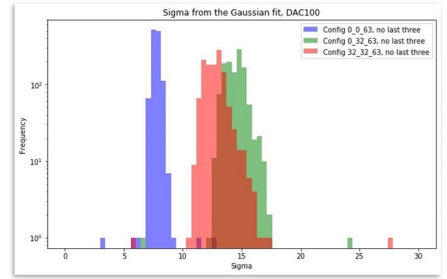
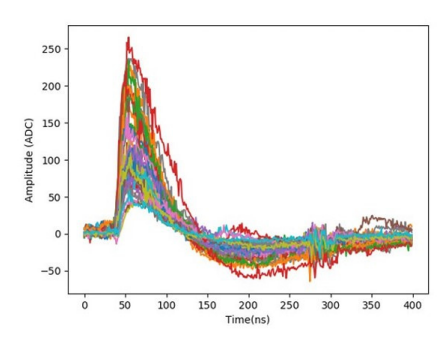


Fig. 5. – Quality control results on the SMART Hodoscope boards. Left: recovery time obtained from the exponential fit for the three considered different SMART configurations. Right: sigma from the gaussian fit for the same SMART configurations

of 80 channels per board: specifically, each board can be used to read out a single view of each ICC layer. Therefore, to cover both the X and Y view of the 4 ICC layer, a total of 8 CsI SMART boards is needed to equip the whole instrument. There is, however, one main difference with respect to the SMART Hodo board: in fact, a fast trigger circuit was added in this board, based on a summer amplifier to provide the sum and shaping for the 16 signals coming from each SMART ASIC. The summed signals are then sent to a discriminator, characterized by a threshold value that can be tuned. The logic OR of the five discriminated signals is then performed and used to generate a FAST trigger signal.

As previously done for the Hodo boards, a prototype board was produced and tested: the SMART inputs were coupled to Hamamatsu SiPMs S13360-3050CS  $3\times3~\mathrm{mm^2}$  operated at 43 V and illuminated with a pulsed LED. The waveforms and charge distributions were acquired and measured by a 16-channel digitizer board based on the CTC ASIC, developed for the Cherenkov Telescope Array Observatory [4] . The CTC output can be seen in Fig.6.

Moreover, the summer amplifier was tested: after feeding the board with a single channel, the SMART and summer amplifier output were acquired at the same time through an oscilloscope. It was then possible, thanks to the high resolution of the SMART signals, to select the individual p.e. peaks and compare them with those coming from



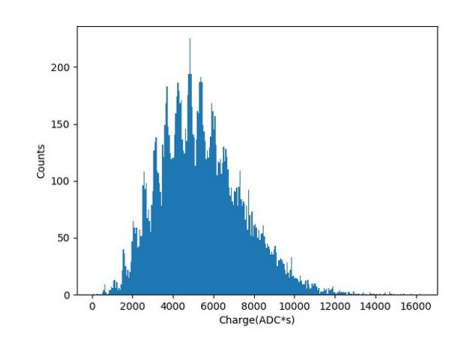


Fig. 6. – Left: waveforms acquired from one SMART channel of the CsI SMART board coupled to a  $3\times3~mm^2$  Hamamatsu SiPMs (S13360-3050 CS) as measured by the 16-channel digitizer board based on the CTC ASIC. Right: the corresponding calculated charge distribution.

the summer amplifier. Fig.7 shows the amplitude distribution from the summer amplifier output: the distributions were then overlaid and only the 1 p.e., 2 p.e. and 3 p.e. events from the SMART outputs were taken into account. The performance of the tested board were in agreement with the design specifications.

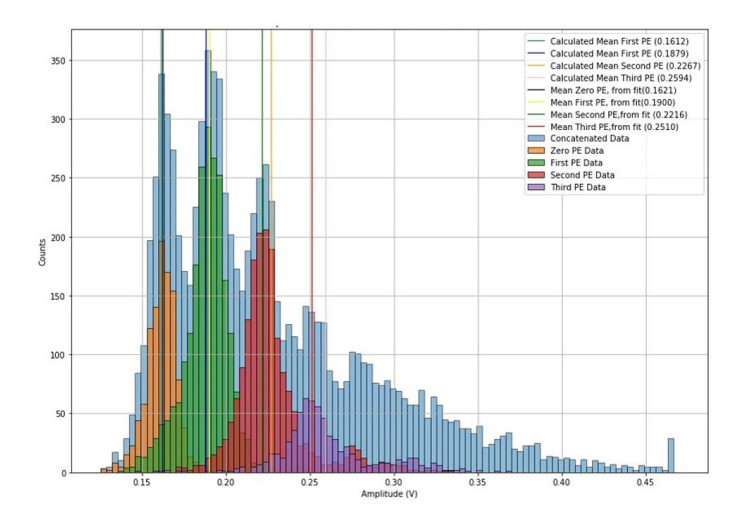


Fig. 7. – Amplitude distribution derived from the summer amplifier output. The orange, green, red and purple distributions identify the 0 p.e., 1 p.e., 2 p.e. and 3 p.e. events selected from the SMART output. The vertical lines show the mean values mean of individual p.e. distributions, both as calculated from the histograms and from a gaussian fit.

After this phase, 11 CsI boards were produced and tested: the inputs of the SMART were coupled to Hamamatsu SiPMs S13360-3050CS  $3\times3$  mm<sup>2</sup> operated at 43V and illuminated with a pulsed LED. The analysis are ongoing, and the integration of the full instrument is expected at the beginning of 2026.

#### 4. - Conclusions

The ADAPT instrument is a demonstrator for the future APT mission. In this work, the structure of the instrument was presented and explained. Moreover, the results of the prototyping phase and quality control of the read-out electronics of two subdetectors, the Hodoscope and ICC, were presented; the main characteristics and validation tests were presented. The production of the boards was completed and integration in the full ADAPT instrument is expected in the second half of 2025.

### 5. - Acknowledgments

This work was supported by NASA award 80NSSC21K1741, NSF award CNS-1763503 and by Istituto Nazionale di Fisica Nucleare (INFN).

#### REFERENCES

- [1] BUCKLEY J. et al., The adapt mission: The antarctic demonstrator for the advanced particle astrophysics, presented at Telescope 20th Divisional Meeting of the High Energy Astrophysics Division, American Astronomical Society 2023.

  URL https://adapt.physics.wustl.edu/
- [2] Sudvarg M. et al., Front-end computational modeling and design for the antarctic demonstrator for the advanced particle-astrophysics telescope, presented at 38th International Cosmic Ray Conference 2023. URL https://doi.org/10.22323/1.444.0764
- [3] ARAMO C. et al., Nuclear Instruments and Methods in Physics Research Section A: Accelerators, Spectrometers, Detectors and Associated Equipment, (2022). URL https://www.sciencedirect.com/science/article/pii/S0168900222011317
- [4] SCHWAB B. et al., Nuclear Instruments and Methods in Physics Research Section A: Accelerators, Spectrometers, Detectors and Associated Equipment, 1069 (2024) 169841. URL https://doi.org/10.1016/j.nima.2024.169841